Journal of Hazardous Materials 170 (2009) 87–95

Contents lists available at ScienceDirect

Journal of Hazardous Materials

journal homepage: www.elsevier.com/locate/jhazmat

Easy extrusion of honeycomb-shaped monoliths using Moroccan natural clays and investigation of their dynamic adsorptive behavior towards VOCs

T. Chafik[a,*], S. Harti[a], G. Cifredo[b], J.M. Gatica[b], H. Vidal[b]

[a] Laboratoire de Génie Chimique et Valorisation des Ressources, Faculté des Sciences et Techniques de Tanger, Université Abdelmalek Essâadi, B.P. 416 Tangier, Morocco
[b] Departamento C.M., I.M. y Química Inorgánica, Universidad de Cádiz, Puerto Real 11510, Spain

ARTICLE INFO

Article history:
Received 22 January 2009
Received in revised form 28 April 2009
Accepted 30 April 2009
Available online 6 May 2009

Keywords:
Clays
Extrusion
Honeycomb monoliths
VOCs
Adsorption

ABSTRACT

In the present work, honeycomb-shaped monoliths were easily extruded using local natural clays without the need of chemical binders. This finding allows significant cost reduction, in terms of not only additives and solvents but also the energy consumption required for their elimination by thermal treatment. The extruded monoliths were subject to mechanical strength testing in addition to the study of their thermal behavior, structural and textural properties. Moreover, one of their potential uses as VOCs adsorbents was evaluated in comparison with conventional packed bed by investigating their dynamic adsorptive and desorption behavior towards a model VOC of o-xylene type.

1. Introduction

Honeycomb-shaped monolith is a uni-body structure composed of parallels cells or channels, commonly made with ceramic such as the most popular cordierite used for three way catalyst [1]. The application of this shape was extended to various environmental issues where large volumetric flow rates, often, have to be handled. This is, mainly, due the open-channel structure that helps eliminating problems associated with pressure drop, especially, when processing effluents containing dust or fly ash, such as the case of power plants emissions treatment with selective catalytic reduction (SCR) [2]. At this regard, honeycomb reactor can provide additional advantage in terms of lower energy consumption, considered as an important part of the overall operating costs, particularly, if there is no economic value created from the gaseous stream treatment process.

The most convenient method for honeycomb monoliths production is based on extrusion of a prepared dye using vacuum presses, followed by drying and thermal treatment [3]. These different steps have to be controlled because they may strongly affect the chemical, catalytic and physical properties as well as the extrudate's morphology, porosity and mechanical strength [4]. The use of permanent and/or temporary binders is, usually, needed and requires adequate mixture of raw material, suitable plasticizing solvent and binders. Therefore, several experiments are necessary to obtain an appropriate composition of paste permitting optimal rheological properties that facilitate extrusion, as recently reported in our previous work [5]. Moreover, the clay's particle size distribution might be adversely affected because of the sintering phenomenon if high temperature is required for additives elimination by thermal treatment [6].

In this work two local natural clays have been used, as raw material, for extrusion of monoliths according to an easy methodology that does not require the use of any chemical additives according to the new concept of 'green chemistry' [7]. The adopted procedure is based on extension of an original method, generally, employed to extrude ceramics. The approach permits to meet adequate plasticity conditions of the pastes allowing extrusion and immediate conformation into rigid structure under honeycomb-shaped monolith [8]. This finding is of interest because it allows combination of several advantages such as those of natural clays cost and physicochemical properties as well as those offered by the use of monolith shape. In addition to further significant saving related with the intrinsic feedstocks price of the chemicals additives used as plasticizers, binders and the energy consumption required for its elimination by thermal treatment. The resulting monoliths were subject to mechanical assays by means of axial crushing strength tests.

The market for ceramic honeycomb monoliths is still under development, not only for environmental applications such as filter and/or catalyst supports but also for various potential uses under development or evaluation in the field of energy, chemical

* Corresponding author. Fax: +212 539 39 39 53.
E-mail addresses: tchafik@yahoo.com, t.chafik@fstt.ac.ma (T. Chafik).

0304-3894/$ – see front matter © 2009 Elsevier B.V. All rights reserved.
doi:10.1016/j.jhazmat.2009.04.127

process, refining industries, catalytic combustion, ozone abatement, etc. [9,10]. In this sense, we investigate one of the potential uses of the extruded clays monoliths as adsorbent for removal of volatile organic compounds (VOCs), together with the study of their structural and textural properties as well as their thermal behavior. Hence, the use of clays monoliths constitutes an attractive option, as most literature devoted to VOCs removal deals with activated carbon monoliths that have been extruded with additives [11–14] or free of binder such as those manufactured by MAST Carbon Ltd., UK [15]. Although activated carbon presents several disadvantages such as flammability risk and pore clog resulting form VOC polymerisation that can be catalyzed by ashes [16]. Therefore, porous materials such as zeolites and clays become interesting alternatives and even more appropriate for VOC removal by adsorption.

As the adsorbent beds are usually operated under dynamic conditions, the evaluation of adsorptive performance of the extruded monoliths, in this work, was achieved through adsorption/desorption experiments carried out under dynamic regime in order to be closer to the real operation conditions. The tests were performed with model-contaminated gaseous stream containing o-xylene that has been selected as representative VOC because it is environmentally relevant regarding local industrial concern.

Thus, the present work could help further development of low cost innovative materials involved in environmental engineering control that could contribute to local sustainable development.

2. Experimental

2.1. Monoliths extrusion and mechanical strength tests

The two raw clay samples to be extruded, hereafter named as FERA and TEFA, were obtained from different deposits located in the north of Morocco. At the beginning, the raw clays were crushed and passed through a 180 μm sieve. Honeycomb monoliths extrusion was achieved following the methodology previously applied for carbon [8] and clay [5]. Accordingly, it is necessary to know the plasticity parameters of the resulting paste, particularly, the liquid limit (LL) and the plasticity index (PI). Briefly, LL corresponds to the amount of water contained in dense liquid when it looses its fluidity (standard procedure UNE 103-103-94), while PI is given by LL–PL, being PL (plastic limit) the water content of a plastic material when it is no more mouldable (standard procedure UNE 103-104-93). A press machine was used for dough extrusion of honeycomb-shaped monoliths with 3×3 configuration. After extrusion and drying overnight at 90 °C, axial crushing strength of the monoliths was measured with a Shimadzu AG-IS Universal Machine for mechanical assays capable of working at a maximum pressure of 100 kN, following the standard procedure UNE-EN ISO 604.

2.2. Characterisation, thermal studies and adsorptive properties

Structural studies were carried out with X-ray diffraction (XRD) at room temperature using a Bruker D8-500 powder diffractometer operating with Cu Kα radiation. The 2θ angle ranged from 14° to 65° with a step of 0.03°/5 s, from 65° to 105° with a step of 0.05° during counting time of 7 s, and from 105° to 145° with a step of 0.07° and a counting time of 9.5 s.

FTIR analysis of clays surfaces were performed with a conventional IR quartz cell equipped with CaF_2 windows allowing treatment of self-supported sample wafers as well as spectra measurements. After evacuation under high vacuum at 200 °C for 30 min, spectra were recorded in absorbance mode, by performing 100 scans from 4000 to 400 cm^{-1} with a resolution of 4 cm^{-1}, using a VERTEX 70 FTIR instrument operated with OPUS software.

Scanning electron microscopy (SEM) images and energy dispersive spectrocopy (EDS) data have been obtained with a QUANTA-200 scanning electron microscope (Philips) equipped with a Phoenix Microanalysis System using a nominal resolution of 3 nm.

Thermogravimetric technique (TGA) was applied to study the thermal evolution of the clays and was carried out under air with a Shimadzu TGA-50 thermobalance using a sample of 20 mg and a heating rate of 10 °C min^{-1}. In order to identify species involved in the studied thermal process, complementary temperature programmed desorption (TPD) experiments were performed using a Pfeiffer Vacuum Balzers mass spectrometer (MS), model QMS 200, operated with Quadstar 32-Bit software for data acquisition and processing. The experiments were carried out with 200 mg of sample heated at a 10 °C min^{-1} rate from room temperature up to 950 °C, under He flow of 60 cm^3 min^{-1}.

Textural characteristics were investigated by means of adsorption/desorption of N_2 at −196 °C, using a Micromeritics ASAP 2020. The experiments were performed with samples which were, first, subjected to heating treatment under high vacuum at 200 °C for 4 h for both raw clays powder and pieces form the crashed extruded monoliths. The isotherms obtained were used to calculate the specific surface area, S_{BET}, and the porosity using the equipment's software.

VOC adsorption/desorption behavior was investigated under dynamic conditions using a homemade apparatus permitting evaluation of amounts involved in adsorption and desorption as previously reported [17]. For this purpose, a model o-xylene/N_2 mixture was prepared by mean of a saturator associated with a condenser that was immersed in a thermostatically controlled bath to keep the temperature at 10 ± 0.5 °C. These conditions lead to a flow stream containing 3600 ppm of xylene in N_2 which has been used with a total flow of 100 cm^3 min^{-1}. The adsorption tests were carried out at 27 °C with samples pre-treated under N_2 flow at 210 °C for 30 min. The adsorbent regeneration behavior was examined by performing desorption experiment, first at 27 °C (isothermal desorption) until the o-xylene concentration at the reactor outlet reached zero. This step was followed by subsequent temperature programmed desorption experiment using a heating rate of 5 °C min^{-1}. An adapted stainless steel reactor was used to perform adsorption/desorption experiments with the extruded monoliths (around 4.5 g) as well as with pellets from crashed monoliths (around 6 g). The gas mixture composition at the reactor outlet, during adsorption or desorption experiments, was monitored by a FTIR spectrometer (Jasco 410, resolution 4 cm^{-1}), using a homemade Pyrex gas cell equipped with CaF_2 windows. Quantitative FTIR data were obtained by integrating the characteristic o-xylene FTIR bands located between 2600 and 3200 cm^{-1}, based on prior calibration performed with mixtures of known o-xylene concentrations. The adsorbed amounts involved in the cycle of successive steps, i.e., adsorption, isothermal desorption and TPD, were obtained by numerical integration with an appropriate software of the areas above the resulting experimental curves giving the evolution of concentration versus time after subtracting the area of experimental curve obtained with empty reactor [18].

3. Results and discussion

3.1. Monoliths extrusion and mechanical strength tests

The clays studied in the present work have been selected considering their low cost (30 €/ton, transportation expenses excluded, according to local estimate) and based on our former experience concerning other local clays extrusion [5]. In contrast with the previous report, honeycomb monoliths were successfully

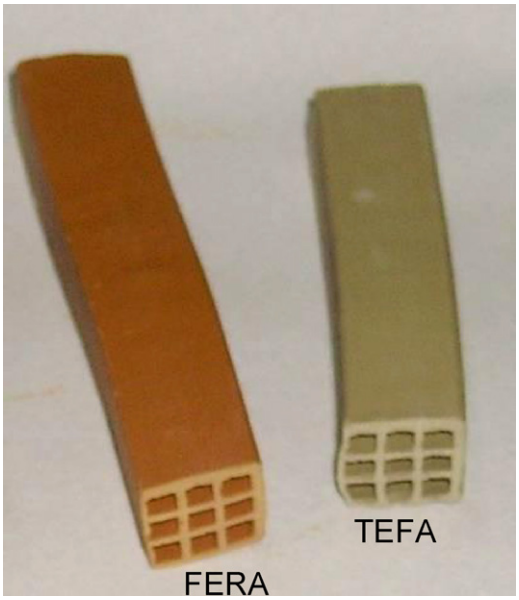

Fig. 1. Monoliths extruded in the laboratory with FERA and TEFA clays.

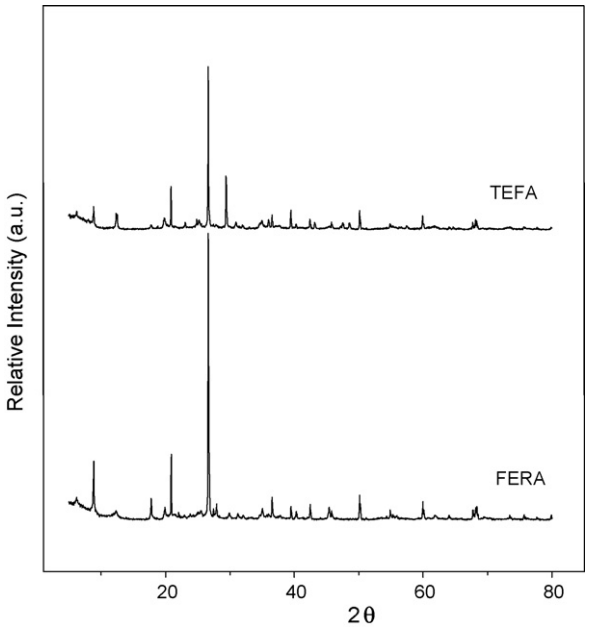

Fig. 2. XRD patterns of FERA and TEFA raw clays (only the 2θ region between 5° and 80° has been represented for shake of clarity).

extruded using natural clays, following the same procedure but without the use of any chemical binder and plasticizer. The paste obtained with the studied clays fulfilled Casagrande's technique [19] requirements, just by adding appropriate amounts of water. The measurement of plastic properties, characterised by liquid limit and plasticity index, leads to values simultaneously located within the frame of 40% < LL < 60% and 10% < PI < 30%. Fig. 1 shows the resulting lab-scale honeycomb monoliths after drying overnight at 90 °C. The extruded monoliths present the following geometric properties; square section of 13.7 cells cm^{-2}, wall thickness of 0.08 cm and geometric surface area of 10.4 cm^2 cm^{-3} with an open frontal area of 49%.

The axial crushing strength measurement performed according to the aforementioned procedure yields to values of mechanical resistance of 2.53 and 1.62 MPa, respectively, for FERA and TEFA. These values are lower than 20.7 MPa obtained, for example, with cordierite type Celcor 9475 from corning glass [2], or those published for ceramic composites [11], carbon-coated cordierite monoliths [14] and those reported for monoliths based on pillared clays [20]. However, the obtained mechanical values are similar [21] or even better than those reported in the literature for integral-type carbon monoliths extruded with binders [22]. It is known that the crushing strength performance strongly depends on the chemical used as binder and the preparation steps performed [2,21]. So far, the measured mechanical resistance of the extruded monoliths might be considered as sufficient for some applications regarding the advantage of their easy preparation free of binder.

3.2. Structure and chemical composition

The X-ray diffractograms of raw clays shown in Fig. 2 gives the mineralogical composition of different phases that have been identified based on the International Centre for Diffraction Data (ICDD) database (Table 1). The obtained data revealed a complex structural heterogeneity corresponding to different laminar phyllosilicates (micas, feldspars, chlorites) as well as quartz and even carbonate containing species such as calcite (case of TEFA clay).

Additional information on clay's surface species was provided by infrared spectroscopy analysis (Fig. 3). Of interest the IR bands detected only in the case of TEFA, located at 2513, 1796 and 1418 cm^{-1} attributed to carbonates species according to the literature

Table 1
Mineralogy information of the studied clays according to the X-ray diffraction analysis (ICCD database PDF code of the phase identified into brackets).

Material	Mineralogical composition
FERA	Quartz (01-087-2096), muscovite (01-087-2096), vermicullite (01-0770022), kaolinite (01-080-0885), albite (00-019-1184)
TEFA	Quartz (01-087-2096), calcite (01-085-1108), muscovite (01-089-6216), clinochlore (01-087-2496)

[23]. These features are related with the presence of calcite phase, in agreement with our XRD data (Table 1). Similar results were reported in the literature for others Moroccan clays from Marrakech area, indicating the presence of carbonate associated with dolomite

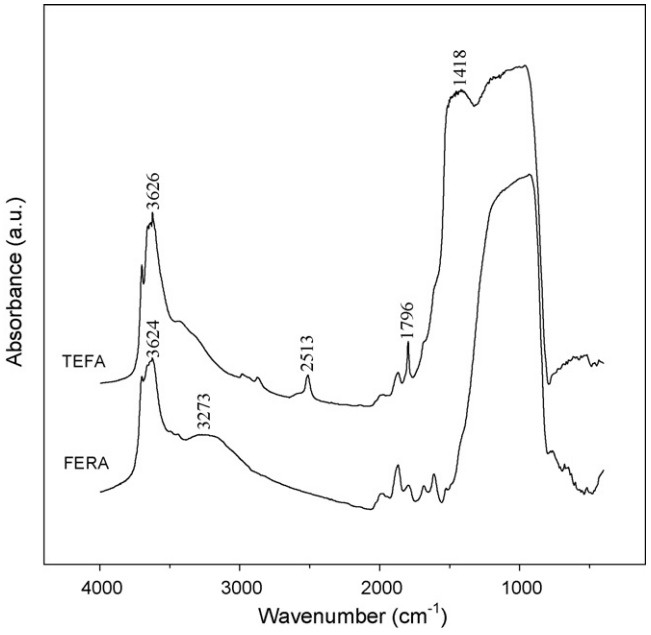

Fig. 3. Fourier transform infrared spectroscopy spectra of the raw FERA and TEFA clays surfaces.

Table 2
Elemental analysis (wt. %) of the studied clays as measured by EDS technique.

Clay	O	Si	Al	C	Na	K	Mg	Ca	Fe	Ti	Cl	S
FERA	39.3	23.4	13.2	0.4	0.3	5.3	0.8	0.6	16.3	0.4	–	–
TEFA	44.4	21.3	9.2	5.1	–	2.8	1.9	5.8	8.9	0.2	0.2	0.2

mineral [24]. Therefore, the infrared bands observed for both samples around 3625 cm^{-1} corresponds to OH stretching vibrations, while the one at 3273 cm^{-1} exhibited by FERA clay only, might be reasonably related with interlayer moisture as pointed out in the literature [25]. This observation would also agree with XRD analysis and could be related with the presence of vermiculite phase in FERA and its absence in TEFA clay (see Table 1).

Complementary microanalysis results obtained by EDS (Table 2) confirm the existence of elements usually contained in aluminosilicate materials. It is worthy noting the lower Si/Al ratio in the FERA sample and the higher carbon content in the TEFA. This is in good agreement with the empirical phase composition suggested by XRD analysis for these minerals, in particular, the detection of more aluminium-rich silicates and calcite (Table 1). Also remarkable, the higher content of iron in the FERA clay, which is consistent with its reddish color in contrast with the greyish color of TEFA.

3.3. Thermal analysis

Thermal behavior of the natural clays was investigated by means of thermogravimetric analysis with particular attention given to the conditions of moisture release. As shown in Fig. 4, the heating process yields to four or five different stages of weight loss depending on the studied clay. The first loss occurs practically from room temperature up to almost 200 °C for both samples, with a maximum at around 90 °C. The second loss is not so well defined and extends up to approximately 300 °C for FERA and up to 400 °C for TEFA. The third stage, denoted by a slighter change in the curve slope, last up to around 500 °C in the case of FERA clay while it goes from 400 to 500 °C for TEFA. Another weight loss exhibited between 500 and 650 °C approximately, is distinguishable by additional slight change in the curve slope. Finally, the last stage in the FERA sample covers a wide thermal range remaining even not concluded by the end of the experiment, whereas appears to be more defined for TEFA, with a maximum rate at 700 °C. The quantitative analysis of the diagrams also indicates that the TEFA sample clearly exhibits a higher total weight loss (almost the double).

Complementary information concerning the species involved in the different weight losses is given by TPD-MS experiments performed under similar heating conditions. Fig. 5 shows the results obtained by monitoring the signals at $m/e = 18$ and $m/e = 44$, corresponding to water and carbon dioxide respectively, these two being the only gaseous products detected. This approach allows the attribution of species involved in the observed weight losses occurring during thermal process and its correlation with TPD data. As seen in Fig. 5, the weight loss at lower temperatures corresponds certainly, as above anticipated with the elimination of moisture typically retained by the surface of a porous material. This process is similar in magnitude for the two studied clays (notice magnification factor for FERA in Fig. 5) and could be considered as a first indication of, relatively, similar surface area. Regarding the second stage above referred, the TPD spectra allow its correlation with water, either, released from the less accessible pores or proceeding from dehydroxylation. According to the XRD analysis (Table 1) and FTIR spectra (Fig. 2), the contribution of water from the hydrated nature of the crystal structure has to be taken into account, especially in the case of FERA for which the presence of vermiculite phase is detected. Above 400 °C, the TPD analysis of the TEFA clay shows the release of both water and CO_2, which is clearly more significant (see the intense peak of CO_2 at 700 °C in Fig. 5). However,

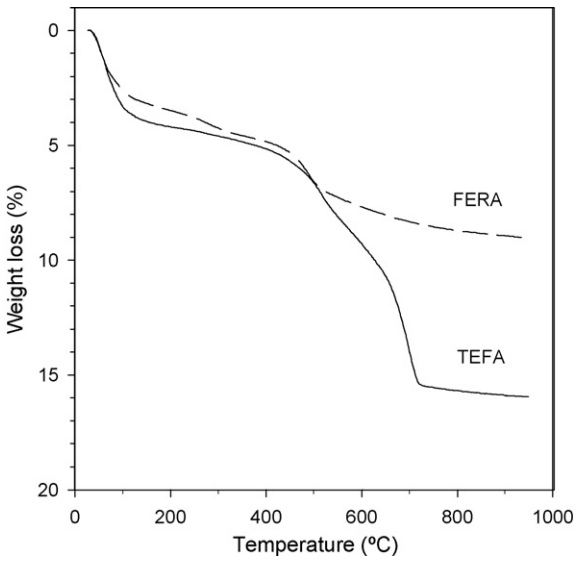

Fig. 4. Thermogravimetric analysis of the raw FERA and TEFA clays.

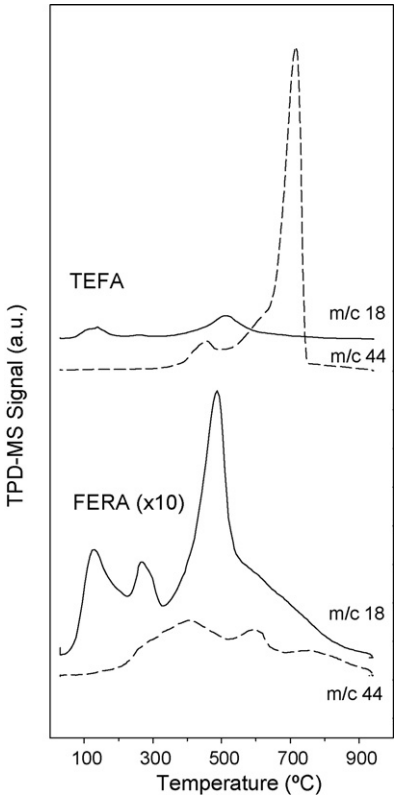

Fig. 5. TPD-MS diagrams of H_2O (m/e: 18) and CO_2 (m/e: 44) obtained with raw FERA and TEFA clays. The diagrams have been corrected considering the mass spectrometer sensitivity to the different species analyzed and have been normalized (notice magnification factors) for comparative purposes.

in the case of FERA there is a release of water, very likely proceeding from further dehydroxylation (see peak at 500 °C) which is relatively more intense than the hardly detected CO_2. This difference can be related with carbonate mineral decomposition process exhibited by TEFA clay, in agreement with the presence of calcite, as indicated by XRD, EDS and FTIR spectroscopy results. Also remarkable, the water desorption from the FERA clay illustrated by TPD $m/e = 18$ signal, occurring almost at the end of the experiment, is in good agreement with the features displayed by ATG diagram at high temperatures (Fig. 4).

The information provided in this section are of interest with respect to extrusion process, particularly, for the needed drying step that requires careful control of the conditions of moisture release together with heating temperature in order to prevent monolith ruptures and cracking.

3.4. Textural characterization

In order to investigate the effect of extrusion on textural characteristics N_2 adsorption and desorption isotherms were measured for the both studied clays with samples of the raw powders and the extruded monoliths (Fig. 6). According to literature classification, the obtained isotherms are of type IV illustrating the presence of larges pores [26,27]. The isotherms adsorption and desorption branches coincide over the interval $0 < P/P_0 < 0.45$, showing N_2 reversible adsorption. After multilayer formation, capillary condensation occurs with progressive filling of all the pores until P/P_0 reaches approximately 0.96, then bulk liquid nitrogen forms at $P/P_0 = 1$. Generally, the involved pores shapes might be cylindrical, parallel-sides silt, wedge, cavity or cone in a bottle. On the other hand, it is known that during adsorption, condensation starts from the narrowest pores while evaporation during desorption begins from the largest pores. This difference is the major cause of the hysteresis between adsorption and desorption isotherms observed above relative pressure of 0.45. Hence, it should be pointed out that besides the relatively similar values of the quantity adsorbed given by the isotherms (Fig. 6), the almost identical hysteresis in shape and extension also suggests a quite similar pore structure for both studied clays. This is confirmed by comparison of the two clays pore size distribution obtained by means of BJH analysis of the isotherms, as shown in Fig. 7A and B. It is clearly observed, although with slight differences in the relative intensity, that both samples present a predominance of larger pore size structure of meso- and macro-pores types at respective average width around 500 and 1000 Å. These results are in agreement with the data processing derived from the isotherms summarized in Table 3, revealing negligible presence of micropores and similar porosity being slightly higher for FERA clay. Although these values are clearly lower than that reported in literature for classical commercial adsorbents, they might be considered as acceptable taking into account that the clays here studied have

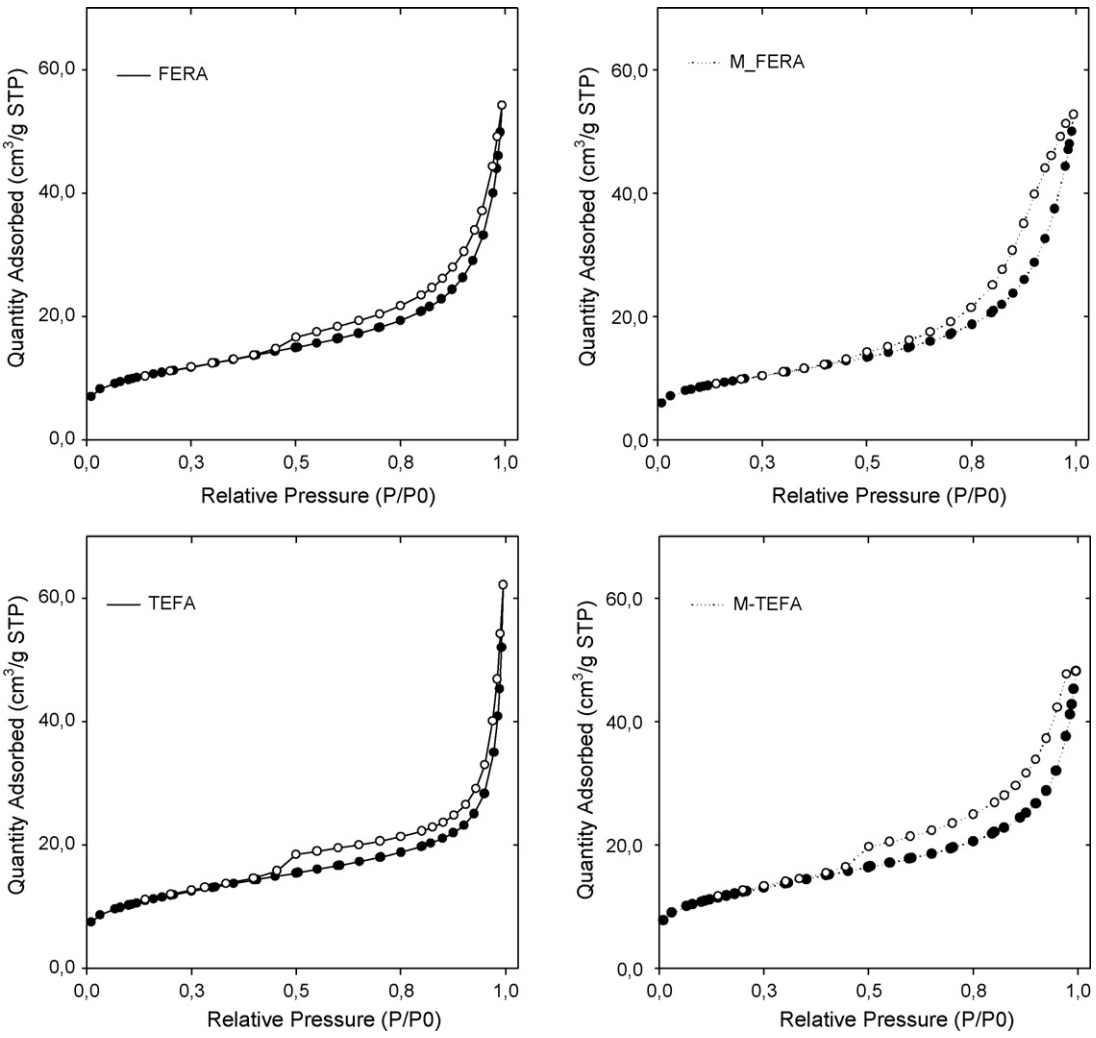

Fig. 6. Nitrogen adsorption desorption isotherms obtained with FERA and TEFA clays before (raw powder) and after monolith extrusion (M). Adsorption (●) and desorption (○) branches are shown.

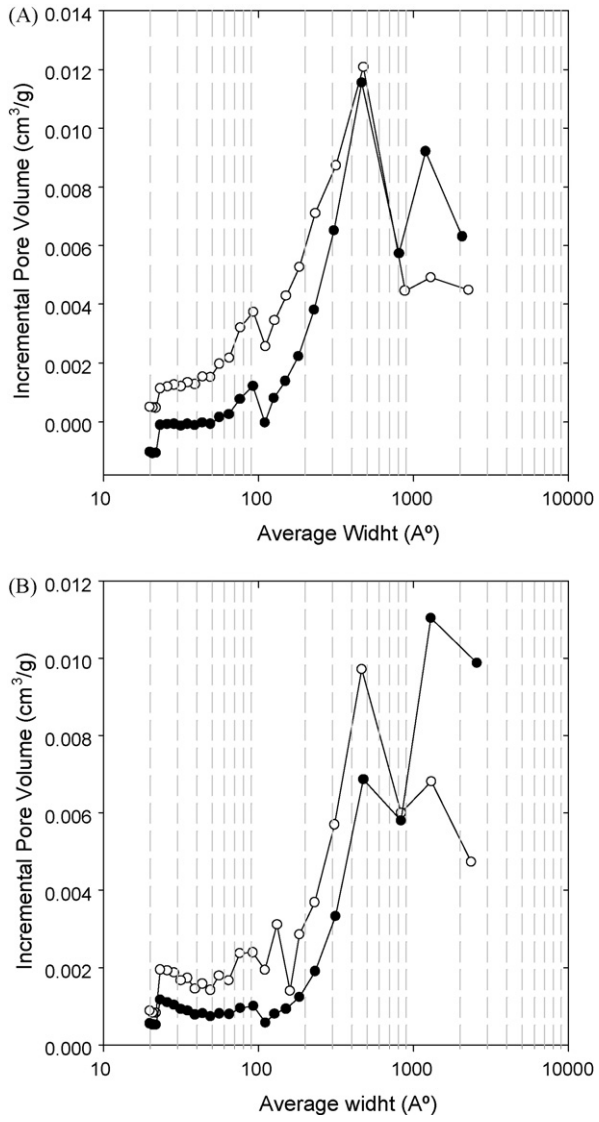

Fig. 7. Pore size distribution for FERA (A) and TEFA(B) clays in the forms of raw powder (●) and extruded monolith (○) as determined by the BJH method using data of nitrogen adsorption desorption isotherms.

not been subjected to any kind of treatment that enhances textural properties as frequently practiced via acid activation [25,28] or chemical modification [29,30]. In addition, the data summarized in Table 3, indicate that no major changes result from the effect of extrusion process on BET surface area and porosity. Whereas more refined analysis through comparison of the pore size distribution before and after extrusion (Fig. 7) shows a slight increase of minor size pores and small decrease for larger-sized pores. This is more pronounced in the case of the TEFA monolith and might justify the small decrease of its total pore volume (Table 3). This result is reasonable and agrees with previous studies in literature according to which extrusion often leads to textural changes because of particles packing which in turn may affect the porosity [4]. Another observation that might be related with the extrusion effect on interparticle porosity existing within the agglomerated particles, is illustrated by the slight difference in the hysteresis width between the isotherms given by the raw powder and extruded monolith of the studied clays (Fig. 6). On the other hand, SEM analysis (Fig. 8) shows an agglomerate of particles of heterogeneous size and irregular shapes for both clays. It is also displayed inter-particle/agglomerate void spaces, which may contribute to porosity as stated above. Nevertheless, these analyses do not reveal any significant textural changes as result of extrusion process.

Table 3
Textural properties of the studied clays investigated by means of N_2 adsorption/desorption isotherms before and after extrusion (raw clay/pellets of extruded monolith).

Sample	BET surface area (m^2/g)	Pore volume (ml/g)	
		Micropores[a]	Total porosity[b]
FERA	38.2/37.7	0.0034/0.0026	0.0712/0.0742
TEFA	40.5/40.4	0.0031/0.0036	0.0700/0.0661

[a] As estimated by means of *t*-plot (Harkins–Jura) analysis.
[b] Single point adsorption total pore volume of pores at $P/P_0 \approx 1$.

3.5. Dynamic adsorption/desorption behavior

Adsorption is a proven chemical engineering method for VOCs removal with the advantage of providing additional benefit in case if valuable solvent recovery is also targeted [31]. Honeycomb monolith reactor is known to be particularly suitable than packed bed system for adsorption processes requiring lower pressure drop [32]. This is mainly due to its higher geometric surface area to volume ratio provided by its open-channel structure capable of processing large gaseous streams.

This section aims at evaluating the dynamic adsorption/desorption performances of the extruded monoliths through determination of the amounts involved in adsorption/desorption and the evolution of adsorbate concentration profile at reactor outlet. These performances were compared to that obtained with pellets from the crashed monoliths because commercial adsorption processes, also, use packed beds. The testing methodology was based on using Fourier transform infrared spectroscopy (FTIR) for measurement of adsorbed and desorbed amounts under dynamic conditions. This approach has been shown to be efficient for distinguishing and quantifying different type of adsorption, in addition to further monitoring of adsorbate transformation through simultaneous detection of new IR bands [17,18,33]. The experiments consist on a cycle of successive steps; adsorption at 300 K until saturation ($N_2 \rightarrow$ o-xylene/N_2, i.e., breakthrough curve) followed by isothermal desorption (o-xylene/$N_2 \rightarrow N_2$) then temperature programmed desorption. Besides the increase and then decrease of o-xylene IR bands respectively during adsorption and desorption steps, the recorded FTIR spectra do not reveal any signs of o-xylene degradation (spectra not shown). The quantitative treatment of the o-xylene IR bands permitted obtaining the variation of its concentration in the gas flow at reactor outlet versus time (Fig. 9A and B) represented as relative values (C_{out}/C_{in}). These curves were, in turn, integrated according to procedure detailed elsewhere [33]. Accordingly, different involved amounts were obtained, i.e., total adsorption Q_{tot} given by the breakthrough curves as well as easily desorbed fraction Q_{rev} (reversible) and more strongly adsorbed fraction Q_{irrev} (considered as irreversible because it is released during TPD). These data are of interest because they permit to evaluate the performance of adsorbent material in terms of adsorption capacity and recovery efficiency, with respect to not only adsorbent regeneration but also to solvent collection for reuse. The measurements were repeated three times in order to check the reproducibility of different results. Hence, the reported data obtained for both pellets and monoliths summarised in Table 4, were found to fit the mass balance equation ($Q_{to} \approx Q_{rev} + Q_{irrev}$) with an experimental deviation less than 5% (the best result of three measurements). Moreover, the monolith performance as indicated by the total adsorption values remains unchanged during the two first tests and suffers small decrease starting from the third reuse.

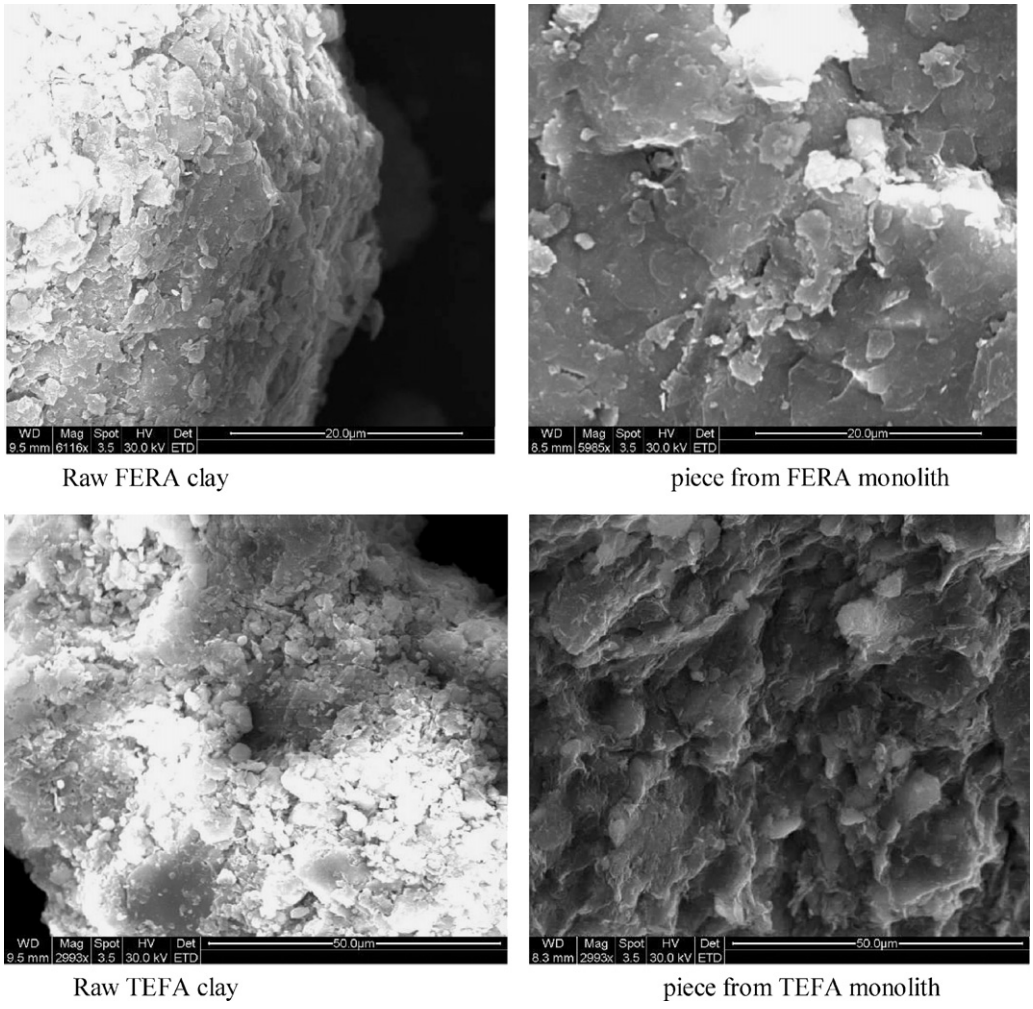

Fig. 8. SEM micrographs obtained with the raw FERA and TEFA clays and pieces from the corresponding extruded monoliths.

The adsorption capacity values were found to be slightly higher for FERA clay, presumably due to its relatively higher pore volume (Table 3), although the slightly higher BET surface of TEFA clay, that may provide better contact efficiencies between adsorbent and flow stream. It is known that the adsorption process occurs, first, through diffusion in macro-pores before adsorbate fixation in the accessible porosity; i.e., inter-particulate as well as meso and/or the micro porosity. The latter parameters, generally, determine the adsorptive capacity of an adsorbent material [13,32]. The obtained adsorption capacities per adsorbent weight were found to be almost similar for the extruded monolith and granular forms of each studied clay. Nevertheless, these values remain lower than those reported for more porous adsorbents, for example, commercial silica [34] or activated carbon monoliths [15,22,35,36].

Also remarkable for both clays, most of the total adsorbed amount (around 78%) corresponds to reversible adsorption released by isothermal desorption. Complete elimination of the more strongly retained fraction in less accessible porosity requires heating at temperatures below 130 °C (see Table 4 and Fig. 9A and B). This is, also, very important from the viewpoint of energy saving since VOC loaded adsorbent are, usually, regenerated by heating. This performance is much better than that reported for carbon-based honeycomb monoliths, requiring temperatures as high as 300 °C to achieve total desorption of adsorbed o-xylene [22].

Table 4
Summary of the measured adsorption/desorption amounts per adsorbent weight (μmol/g) obtained with extruded monolith (M) and crashed monolith pellets (CM).

Clay	Total adsorption	Reversible fraction	Irreversible fraction	T_m
M_FERA	144.474	107.487	34.12	130
CM_FERA	143.92	103.72	34.71	120
M_TEFA	140.132	109.735	29.64	120
CM_TEFA	140.82	105.47	31.41	115

The breakthrough curves profile exhibited by the extruded monolith and pellets of crashed monolith (Fig. 9A and B) show different dynamic adsorption behavior. This illustrates, as expected, the influence of different dynamic mass transfer process during the gas passage along the monolith as compared to the packed bed. In deed, the external mass transfer within the honeycomb channels follows laminar mode with radial diffusion of reactant from bulk fluid phase to the surface of monolith walls which depend on channel diameter, whereas different external diffusion regime exists throughout the granules of packed bed [37]. Therefore, similar internal diffusion process is expected to occur within the porous structure of crashed monoliths pieces and the walls of extruded monolith.

On the other hand, the adsorption experiments reveal shorter breakthrough time for the monoliths as compared with the packed bed (Fig. 9A and B). However, the latter is known to presents several practical drawbacks under industrial conditions (i.e., less fluid stream accessibility to adsorbent due to the preferential flow patterns that may be established across the packed bed, higher pressure drop associated with the flow) [32]. The use of honeycomb

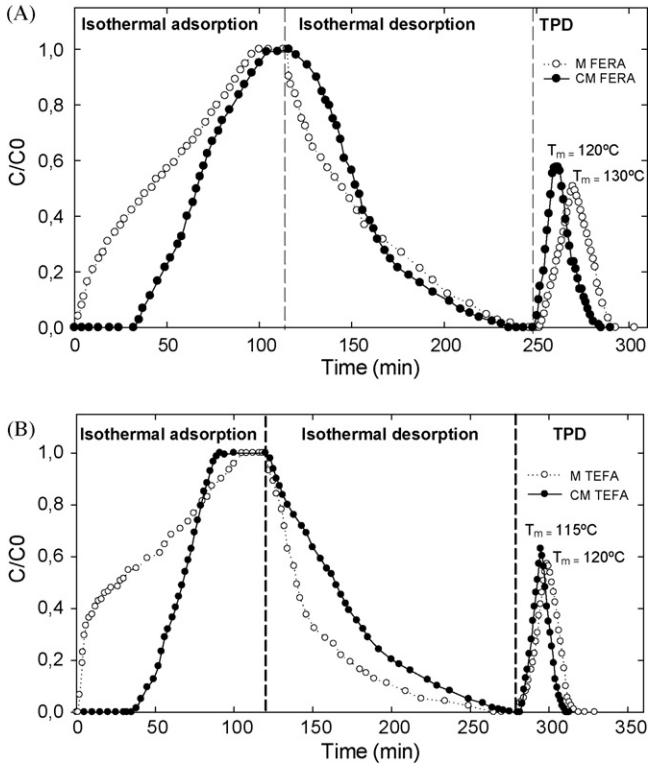

Fig. 9. Profiles of the variation of o-xylene concentration in the gas flow at reactor outlet (C), represented as relative values (C/C_0), obtained with (M) extruded monolith (≈4.5 g) and (CM) pellets of crashed monolith (≈6 g), respectively for FERA (A) and TEFA (B) clays, during a cycle of successive steps; adsorption performed with a mixture C_0 of 0.36% xylene in N_2 at 27 °C until saturation followed by isothermal desorption than temperature programmed desorption carried out with a linear heating rate of 5 °C/min.

structure allows overcoming these limitations but at the same time may result in lower overall adsorption efficiency. Longer time to breakthrough the monolith needs improvement of external mass transfer, which can be provided with narrower channels. This issue needs further work on monolith design that matches the specific requirement of the targeted application.

4. Conclusions

In the present study, honeycomb-shaped monoliths were successfully extruded from cheap local natural clays without the use of any chemicals binder and plasticizers, offering significant economic impact in terms of additives feedstocks and the energy needed for their elimination. In addition, the finding is of interest because it fits the recent green chemistry concept, which is nowadays, more and more required in production processes involving chemistry. Moreover, the monolith extrusion and conformation into rigid structures was achieved through moderate thermal drying and yields to mechanical strength and geometrical properties that might be sufficient for VOC elimination by adsorption.

Textural analysis of the raw clays reveals the existence of relatively large pores, negligible microporosity and BET surface value around 40 m^2/g that remains unchanged after monolith extrusion. Although these textural properties could not compete with those of activated carbon, the most applicable adsorbent for VOC removal, the use of clay monoliths allow, VOC retention with, mainly, weak physical adsorption that permits easier solvent recovery and adsorbent regeneration with less energy consumption. Nevertheless, monoliths extrusion with narrower channels is still needed in order to enhance the overall adsorption efficiency in terms of breakthrough time. This may help to take benefit of the important advantage of the clay monolith over activated carbon adsorbent with respect to safety operation permitting suppression of fire hazard.

Acknowledgements

The authors appreciate the financial help of the Spanish International Cooperation Agency (AECI projects A/4870/06 & A/8880/07), the Ministry of Science and Innovation through the EU/FEDER Program (Project MAT2008-00889/NAN) and the University Abdelmalek Essaadi for the acquisition of Micromeritics ASAP 2020.

References

[1] R.M. Heck, R.J. Farrauto, S.T. Gulati, Catalytic Air Pollution Control: Commercial Technology, John Wiley and Sons, New York, 2002.
[2] A. Cybulski, J.A. Moulijn, Monoliths in heterogeneous catalysis, Catal. Rev. 36 (2) (1994) 179–270.
[3] P. Avila, M. Montes, E. Miró, Monolithic reactors for environmental applications. A review on preparation technologies, Chem. Eng. J. 109 (2005) 11–36.
[4] P. Forzatti, D. Ballardini, L. Sighicelli, Preparation and characterization of extruded monolithic ceramic catalysts, Catal. Today 41 (1998) 87–94.
[5] S. Harti, G. Cifredo, J.M. Gatica, H. Vidal, T. Chafik, Physicochemical characterization and adsorptive properties of some Moroccan clay minerals extruded as lab-scale monoliths, Appl. Clay Sci. 36 (2007) 287–296.
[6] B. Velde, Introduction to Clay Minerals Chemistry, Origin Uses and Environmental Significance, first ed., Chapman and Hall, London, 1992.
[7] T. Chafik, J.M. Gatica, H. Vidal, G. Cifredo, S. Harti, H. Zaitan, Spanish Patent ES2296521-A1 PCT extended WO2007135212-A1.
[8] J.M. Gatica, J.M. Rodríguez-Izquierdo, D. Sánchez, C.O. Ania, J.B. Parra, H. Vidal, Extension of preparation methods employed with ceramic materials to carbon honeycomb monoliths, Carbon 42 (2004) 3251–3254.
[9] T.A. Boger, A. Heibel, C. Sorensen, Monolithic catalysts for the chemical industry, Ind. Eng. Chem. Res. 43 (16) (2004).
[10] V. Tomašic, F. Jovic, State-of the art in the monolithic catalysts/reactors, Appl. Catal. A 311 (2006) 112–121.
[11] M. Yates, J.A. Martin, M.A. Martin-Luengo, J. Blanco, Study of the efficiency of monolithic activated carbon adsorption units, Stud. Surf. Sci. Catal. 160 (2007) 583–590.
[12] L. Liu, Z. Liu, J. Yang, Z. Huang, Z. Liu, Effect of preparation conditions on the properties of a coal-derived activated carbon honeycomb monolith, Carbon 45 (14) (2007) 2836–2842.
[13] A.B. Fuertes, G. Marbán, D.M. Nevskaia, Adsorption of volatile organic compounds by means of activated carbon fibre-based monoliths, Carbon 41 (2003) 87–96.
[14] F.D. Yu, L. Luo, G. Grevillot, Electrothermal swing adsorption of toluene on an activated carbon monolith. Experiments and parametric theoretical study, Chem. Eng. Process 46 (2007) 70–81.
[15] B. Crittenden, A. Patton, C. Jouin, S. Pereda, S. Tennison, J.A. Botas Echevarria, Carbon monoliths: a comparison with granular materials, Adsorption 11 (2005) 537–541.
[16] S.W. Blocki, Hydrophobic zeolite adsorption: a proven advancement in solvent separation technology, Environ. Prog. 12 (1993) 226–237.
[17] H. Zaitan, T. Chafik, FTIR determination of adsorption characteristics for volatile organic compounds removal on diatomite mineral compared to commercial silica, C. R. Chimie 8 (2005) 1701–1709.
[18] H. Zaitan, D. Bianchi, O. Achak, T. Chafik, A comparative study of the adsorption and desorption of o-xylene onto bentonite clay and alumina, J. Hazard. Mat. 153 (2008) 852–859.
[19] E. Gippini, Pastas Cerámicas, Sociedad Española de Cerámica, Madrid, 1979.
[20] F. Mohino, A.B. Martin, P. Salerno, A. Bahamonde, S. Mendioroz, High surface area monoliths based on pillared clay minerals as carriers for catalytic processes, Appl. Clay Sci. 29 (2005) 125–136.
[21] T. Vergunst, M.J.G. Linders, F. Kapteijn, J.A. Moulijn, Carbon-based monolithic structures, Catal. Rev. 43 (3) (2001) 291–314.
[22] J.M. Gatica, J.M. Rodríguez-Izquierdo, D. Sánchez, T. Chafik, S. Harti, H. Zaitan, H. Vidal, Originally prepared carbon-based honeycomb monoliths with potential application as VOCs adsorbents, C. R. Chimie 9 (2006) 1215–1220.
[23] K. Nakamoto, Infrared and Raman Spectra of Inorganic Coordination Compounds, third ed., John Wiley and Sons, New York, 1977.
[24] A. Alami, M. Boulmane, M. Hajjaji, S. Kacim, Chemico-mineralogical study of a Moroccan clay, Annales de Chimie-Science des Materiaux 23 (1998) 173–176.
[25] G.E. Christidis, P.W. Scott, A.C. Dunham, Acid activation and bleching capacity of bentonites from the islands of Milos and Chios, Aegean, Greece, Appl. Clay Sci. 12 (1997) 329–347.
[26] S.J. Greig, S.W. Sing, Adsorption, Surface Area and Porosity, Academic Press, London, 1982.
[27] K. Sing, The use of nitrogen adsorption for characterization of porous materials, Colloid Surf. A: Phys. Eng. Aspects 3–9 (2001) 187–188.

[28] H. Noyan, M. Onal, Y. Sarıkaya, The effect of sulphuric acid activation on the crystallinity, surface area, porosity, surface acidity, and bleaching power of a bentonite, Food Chem. 105 (2007) 156–163.
[29] R. Mahboub, Y. El Mouzdahir, A. Elmchaouri, A. Carvalho, M. Pinto, J. Pires, Characterization of a delaminated clay and pillared clays by adsorption of probe molecules, Colloids Surf. A: Phys. Eng. Aspects 280 (2006) 81–87.
[30] J. Pires, M. Bestilleiro, M. Pinto, A. Gil, Selective adsorption of carbon dioxide, methane and ethane by porous clays heterostructures, Sep. Purif. Technol. 61 (2007) 161–167.
[31] F.I. Khan, A.K. Goshal, Removal of volatile organic compounds from polluted air, J. Loss Prev. Process Ind. 13 (2000) 527–545.
[32] D.M. Ruthven, Past progress and future challenges in adsorption research, Ind. Eng. Chem. Res. 39 (2000) 2127–2131.
[33] T. Chafik, H. Zaitan, S. Harti, A. Darir, O. Achak, Determination of the heat of adsorption and desorption of a VOC under dynamic conditions using Fourier transform-infrared spectroscopy, Spectro. Lett. 40 (2007) 763–775.
[34] K. Kosuge, S. Kubo, N. Kikukawa, M. Takemori, Effect of pore structure in mesoporous silicas on VOC dynamic adsorption/desorption performance, Langmuir 23 (2007) 3095–3102.
[35] C. Wang, K. Chang, K.T. Chung, Adsorption equilibria of aromatic compounds on activated carbon, silica gel and 13X zeolite, J. Chem. Eng. Data 49 (2004) 527–531.
[36] M.S. Balathanigaimani, S. Wang-Geun, L. Min-Joo, L. Jae-Wook, M. Hee, Adsorption isotherms of benzene and toluene on corn grain-based Carbon monolith at (303.15, 313.15, and 323.15 K), J. Chem. Eng. Data 5 (2008) 732–736.
[37] F. Kapteijn, J.A. Moulijn, in: G. Ertl, H. Knözinger, J. Weitkamp (Eds.), Handbook of Heterogeneous Catalysis, vol. 3, VCH, Weinheim, 1997, pp. 1359–1376.